2021 61st IEEE Conference on Decision and Control (CDC)
December 6-9, 2022. Cancún, Mexico

Bi-SIS Epidemics on Graphs - Quantitative Analysis of Coexistence Equilibria

Vishwaraj Doshi*, Jie Hu*, and Do Young Eun

***Abstract*— We consider a system in which two viruses of the *Susceptible-Infected-Susceptible* (SIS) type compete over general, overlaid graphs. While such systems have been the focus of many recent works, they have mostly been studied in the sense of convergence analysis, with no existing results quantifying the non-trivial coexistence equilibria (CE) - that is, when both competing viruses maintain long term presence over the network. In this paper, we prove monotonicity of the CE with respect to effective infection rates of the two viruses, and provide the first quantitative analysis of such equilibria in the form of upper bounds involving spectral radii of the underlying graphs, as well as positive equilibria of related single-virus systems. Our results provide deeper insight into how the long term infection probabilities are affected by system parameters, which we further highlight via numerical results.**

I. Introduction

The study of multiple competing viruses over graph topologies has gained considerable traction in recent years [1]–[3]. This is mainly because of their versatility in modeling not just infectious diseases, but also phenomena such as opposing views and opinions [4] and competing products [5]. These phenomena, which we will commonly refer to as *epidemics* or *viruses*, spread over topologies such as social networks and other media platforms, word of mouth, or even human contact - often modelled as graphs with edges representing the way we connect with one another.

Due to the relative ease of analysis, the *bi-virus* model of competition between *two* epidemics has seen more profound analysis [6]–[11], the underlying viruses typically being of the *Susceptible-Infected-Susceptible* (SIS) type. The original (single virus) SIS model on graph was introduced to model the spread of Gonorrhea in [12], which also provided the complete convergence characterization. Two outcomes were shown to be possible - either the virus persists over the network in the long run, when the *effective infection rate* $\tau > 0$ is larger than a certain threshold value $\tau^* > 0$, or the virus dies out and the system converges to a healthy state when $\tau^* \leq 0$.[1]

This threshold conditions for the single-virus SIS model were also independently rediscovered [13], [14], with follow-up works [15], [16] being successful in establishing quantitative bounds on the long run infection probabilities/market share/influence in the case when the virus/product/opinion persists, even showing convexity of the average infection probabilities in $1/\tau$ in some cases [14]. The convergence of the system itself has been proved multiple times in the literature [17]–[19] utilizing techniques other than the original Lyapunov based analysis in [12]. One such convergence proof [20] relies on showing that the SIS epidemic model is a *monotone dynamical system* (MDS); using proof techniques that leverage the convergence properties of monotone sequences in compact sets to extract the threshold criterion.

Recently, MDS techniques were used to establish, for the first time, the complete convergence criterion for the *bi-SIS* model - involving two viruses of the SIS type competing on general, overlaid graphs [21]; providing threshold type conditions under which both viruses (which we refer to as Virus 1 and 2) die out, or one prevails over the other. More interestingly, they were used to establish necessary and sufficient conditions for the existence and global convergence of the system to the set of *coexistence equilibria* (CE), where both viruses maintain presence over the network in the long run - previously an open problem [10]. Recent works [8] also improved the qualitative understanding of the CE by showing that they are always disjoint and finitely many, except for some pathological examples.[2] However, apart from a few results which are simply by-products of the techniques utilized for the convergence proofs in [8], [21], there is a lack of quantitative bounds on CE, and little understanding of their monotonicity properties with respect to the system parameters.

In this paper, we provide quantitative results characterizing the behaviour of CE of the bi-SIS model on general graphs with respect to effective infection rates τ_1, τ_2 of the two competing viruses. Building upon crucial observations obtained via fixed point analysis of the bi-virus system in the MDS framework, we provide new results on the relationship between the long run probability of being infected by Virus 1 versus that of Virus 2, with regards to change in system parameters τ_1, τ_2. These results are sharper than those emerging out of mere convergence analysis, and enable us to further quantify the connection between the CE and the positive equilibrium of corresponding single-SIS models, as well as the spectral radius of the underlying graphs in the form of various upper bounds. We also briefly show via numerical results that the upper bounds are successful in capturing the

*Equal contributors.

Vishwaraj Doshi is with the Data Science and Advanced Analytics team at IQVIA. The research was conducted while he was with the Operations Research Graduate Program, North Carolina State University, Raleigh, NC 27606 (NCSU). Jie Hu and Do Young Eun are with the Department of Electrical and Computer Engineering, NCSU. Email: vishwaraj.doshi@iqvia.com, {jhu29, dyeun}@ncsu.edu. This work was supported in part by National Science Foundation under Grant Nos. CNS-2007423, IIS-1910749, and CNS-1824518.

[1]The effective infection rate $\tau \triangleq \beta/\delta$, where $\beta > 0$ is the infection rate of the virus and $\delta > 0$ stands for the recovery rate from the virus, captures the overall *strength* of a virus.

[2]When the system parameters lie in an algebraic set of measure zero.

trend in which the CE fixed points change with the system parameters. Our results provide a deeper understanding of how the increase (decrease) in strength of one virus affects the presence of its competitor over the network, showing that the expected decrease (increase) can be more drastic than one would expect.

The rest of the papers is organized as follows. In Section II, we give succinct overview on bi-SIS model with a summary of existing convergence results. Section III contains our main results of the paper, with the proofs deferred to the Appendices. We then provide brief numerical results in Section IV, followed by the conclusion.

II. Bi-SIS Epidemic Model - A Primer

A. Basic Notations

We use lower case, bold-faced letters to denote column vectors $\mathbf{v} \in \mathbb{R}^N$, and upper case, bold-faced letters to denote square matrices $\mathbf{M} \in \mathbb{R}^{N\times N}$. We denote by $\lambda(\mathbf{M})$ the spectral radius of a non-negative matrix $\mathbf{M}$. We use $\text{diag}(\mathbf{v})$ to denote the $N \times N$ diagonal matrix with entries of vector $\mathbf{v} \in \mathbb{R}^N$ on the main diagonal, and $\mathbf{1/0}$ for all one/zero vectors with appropriate dimensions. We write $[\mathbf{x}]_i$ or normal letter x_i with index i to represent the i-th entry of vector $\mathbf{x}$. For vectors, $\mathbf{x} \leq \mathbf{y}$ means $x_i \leq y_i$ for all i; $\mathbf{x} < \mathbf{y}$ if $\mathbf{x} \leq \mathbf{y}$ and $\mathbf{x} \neq \mathbf{y}$; $\mathbf{x} \ll \mathbf{y}$ if $x_i < y_i$ for all i. Let $\mathcal{G}(\mathcal{N}, \mathcal{E})$ denote a general, undirected and connected graph with its adjacency matrix $\mathbf{A} = [a_{ij}]$, where $a_{ij} = \mathbb{1}_{(i,j)\in\mathcal{E}}$ for any $i, j \in \mathcal{N}$.

B. The Bi-SIS Model

We consider the spread of Virus 1 and 2 on overlaid graphs $\mathcal{G}_1(\mathcal{N}, \mathcal{E}_1)$ and $\mathcal{G}_2(\mathcal{N}, \mathcal{E}_2)$ respectively, sharing the same set of nodes $\mathcal{N}$, but different edge sets $\mathcal{E}_1$ and $\mathcal{E}_2$ through which the respective epidemics propagate.[3] At any given time, a node $i \in \mathcal{N}$ is either *susceptible*, or is *infected by either Virus 1 or Virus 2*. If infected by Virus 1, the node infects each its susceptible neighbors with rate $\beta_1 > 0$, where neighbors are determined with respect to the edge set $\mathcal{E}_1$ of the graph $\mathcal{G}_1(\mathcal{N}, \mathcal{E}_1)$. Virus 2 is transmitted similarly with rate $\beta_2 > 0$ through the edge set $\mathcal{E}_2$. Also, infected nodes recover with rates $\delta_1, \delta_2 > 0$ depending on whether they are infected by Virus 1 or 2 respectively. We call $\tau_1 \triangleq \beta_1/\delta_1$ and $\tau_2 \triangleq \beta_2/\delta_2$ as the effective infection rates of two corresponding viruses. The system dynamics are described by the following set of ordinary differential equations (ODEs):

$$\begin{aligned}\dot{x}_i(t) &= \beta_1(1 - x_i(t) - y_i(t)) \sum_{j\in\mathcal{N}} a_{ij}x_j(t) - \delta_1 x_i(t),\\ \dot{y}_i(t) &= \beta_2(1 - x_i(t) - y_i(t)) \sum_{j\in\mathcal{N}} b_{ij}y_j(t) - \delta_2 y_i(t)\end{aligned} \tag{1}$$

for all $i \in \mathcal{N}$, where $x_i(t), y_i(t) \in [0, 1]$ are the probabilities that node $i \in \mathcal{N}$ is infected by Virus 1 or 2 respectively at any time $t \geq 0$. Note that $x_i(t) + y_i(t) \in [0, 1]$ at all time.

[3]Using overlaid graphs with different edge sets $\mathcal{E}_1$ and $\mathcal{E}_2$ model the different media through which epidemics, opinions, malware and other such phenomena propagate.

In a matrix-vector form, (1) can be written as

$$\begin{aligned}\dot{\mathbf{x}} &= \beta_1 \text{diag}\,(\mathbf{1} - \mathbf{x} - \mathbf{y})\,\mathbf{A}\mathbf{x} - \delta_1\mathbf{x},\\ \dot{\mathbf{y}} &= \beta_2 \text{diag}\,(\mathbf{1} - \mathbf{x} - \mathbf{y})\,\mathbf{B}\mathbf{y} - \delta_2\mathbf{y},\end{aligned} \tag{2}$$

where $\mathbf{A} = [a_{ij}]$ and $\mathbf{B} = [b_{ij}]$ are the adjacency matrices of the overlaid graphs $\mathcal{G}_1(\mathcal{N}, \mathcal{E}_1)$ and $\mathcal{G}_2(\mathcal{N}, \mathcal{E}_2)$, respectively. We denote by $E \subset [0, 1]^{2N}$ the set of all possible equilibria of system (2), which trivially contains $(\mathbf{0}, \mathbf{0})$.

The *single-SIS* dynamics for Virus 1 can be obtained by setting $\mathbf{y} = 0$ in (2), and is given by

$$\dot{\mathbf{x}} = \beta_1 \text{diag}\,(\mathbf{1} - \mathbf{x})\,\mathbf{A}\mathbf{x} - \delta_1\mathbf{x}. \tag{3}$$

When $\tau_1 > \tau_1^* = 1/\lambda(\mathbf{A})$, any trajectory of the system starting from $[0, 1]^N \backslash \{\mathbf{0}\}$ converges to a positive equilibrium $\mathbf{x}^* \gg \mathbf{0}$, otherwise they converge to $\mathbf{0}$ [12]. Similarly, single-SIS model for Virus 2 can be obtained by substituting $(\beta_2, \delta_2, \mathbf{B})$ for $(\beta_1, \delta_1, \mathbf{A})$ in (3), with its positive equilibrium $\mathbf{y}^* \gg \mathbf{0}$ when $\tau_2 > \tau_2^* = 1/\lambda(\mathbf{B})$.

A preliminary result for bi-SIS epidemics [10] is that any virus which fails to satisfy its respective single-SIS survival threshold will die out in the long run; that is, Virus 1 (Virus 2) will die out irrespective of the presence of its competing virus if $\tau_1 \leq 1/\lambda(\mathbf{A})$ ($\tau_2 \leq 1/\lambda(\mathbf{B})$). If, at any given time $s \geq 0$, a trajectory of (2) enters the sets $[0, 1]^N \times \{\mathbf{0}\}$ (Virus 2 dies out) or $\{\mathbf{0}\} \times [0, 1]^N$ (Virus 1 dies out), it remains in that set for all times $t > s$, and the bi-SIS model effectively reduces to a single-SIS model corresponding to the surviving virus, whose long run behaviour is governed by the single-virus convergence criterion as outlined earlier.

The non-trivial case arises when both $\tau_1 > 1/\lambda(\mathbf{A})$ and $\tau_2 > 1/\lambda(\mathbf{B})$, for which the techniques used to derive the single-SIS convergence criterion no longer apply. Specifically, both positive equilibria of the related single-virus systems $\mathbf{x}^*, \mathbf{y}^* \gg \mathbf{0}$ may exist, and it is only under this scenario when the system can possibly converge to one of (finitely) many *coexistence equilibria* of the kind $(\hat{\mathbf{x}}, \hat{\mathbf{y}}) \gg (\mathbf{0}, \mathbf{0})$. The complete convergence criterion derived in [21] does include the case when $\tau_1 > 1/\lambda(\mathbf{A})$ and $\tau_2 > 1/\lambda(\mathbf{B})$, and gives the following additional conditions on τ_1, τ_2 and the respective outcomes:

(C1) If $\tau_1\lambda(\text{diag}(\mathbf{1}-\mathbf{y}^*)\mathbf{A}) > 1$ and $\tau_2\lambda(\text{diag}(\mathbf{1}-\mathbf{x}^*)\mathbf{B}) \leq 1$, the bi-SIS system (2) converges to $(\mathbf{x}^*, \mathbf{0})$;

(C2) If $\tau_1\lambda(\text{diag}(\mathbf{1}-\mathbf{y}^*)\mathbf{A}) \leq 1$ and $\tau_2\lambda(\text{diag}(\mathbf{1}-\mathbf{x}^*)\mathbf{B}) > 1$, the bi-SIS system (2) converges to $(\mathbf{0}, \mathbf{y}^*)$;

(C3) If $\tau_1\lambda(\text{diag}(\mathbf{1}-\mathbf{y}^*)\mathbf{A}) > 1$ and $\tau_2\lambda(\text{diag}(\mathbf{1}-\mathbf{x}^*)\mathbf{B}) > 1$, the bi-SIS system (2) converges to one CE fixed point $(\hat{\mathbf{x}}, \hat{\mathbf{y}}) \gg (\mathbf{0}, \mathbf{0})$ in the equilibria set E;

Note that in (C1)–(C3), $\mathbf{x}^*$ and $\mathbf{y}^*$ are the single-virus fixed points as defined earlier in the subsection.

Since our focus is quantitative characterization of CE fixed points, in the rest of this paper, we will assume that τ_1, τ_2 always satisfy $\tau_1 > 1/\lambda(\mathbf{A})$ and $\tau_2 > 1/\lambda(\mathbf{B})$ and condition (C3), unless mentioned otherwise.

III. Quantitative analysis of the Bi-SIS model

Before presenting our results for the bi-SIS case, we give a bound on the positive equilibria for single-virus SIS models.

Proposition 1. *Consider the single-virus SIS system* (3)*, and let* $\tau_1 > 1/\lambda(\mathbf{A})$ *with* $\mathbf{x}^* \gg \mathbf{0}$ *being the corresponding positive, globally attractive equilibrium. Then, we have*

$$\frac{\mathbf{1}^T\mathbf{x}^*}{N} \leq 1 - \frac{1}{\tau_1\lambda(\mathbf{A})} \leq x^*_{\max} \triangleq \max_{i\in\mathcal{N}} x^*_i. \tag{4}$$

This upper bound on the average infection probability $\mathbf{1}^T\mathbf{x}^*/N$ in (4) has also been alluded to in [16] as emerging out of the convexity of $\mathbf{x}^*$ in $1/\tau_1$ [14]. Here, we present a formal statement for the bound in the form of Proposition 1, providing a more direct proof using the Fortuin–Kasteleyn–Ginibre (FKG) and Jensen's inequalities in Appendix I, without the need of first showing convexity via lengthy computations. Our approach also allows us to provide the lower bound on the largest entry of $\mathbf{x}^*$, the second inequality in (4).

For regular graphs (with degree d for every node), both the inequalities in (4) become equality since we know from Lemma 7 [15] that $\mathbf{x}^*_i = 1 - 1/\tau_1 d$ for each $i \in \mathcal{N}$, and $\lambda(\mathbf{A}) = d$. When τ_1 is only slightly larger than the threshold $1/\lambda(\mathbf{A})$, intuitively speaking, the virus should not infect a large portion of the network, since it is barely strong enough to survive. The first inequality in (4) confirms this intuition since $\mathbf{1}^T\mathbf{x}^*/N$ is still close to zero for such τ_1, implying that the virus barely survives in the long run. If τ_1 is very large, or $1/\tau_1\lambda(\mathbf{A}) \to 0$, the upper bound of $\mathbf{1}^T\mathbf{x}^*/N$ in (4) gets closer to 1 and doesn't tell much information about $\mathbf{x}^*$. From (4), however, the node with largest infection probability has $x^*_{\max} \to 1$, showing that the virus has at least infected the 'weakest' node in the network that is susceptible to infection.

We now provide quantitative results for the bi-SIS CE fixed points. A CE fixed point $(\hat{\mathbf{x}}, \hat{\mathbf{y}}) \gg (\mathbf{0}, \mathbf{0})$ of system (2) satisfies the following equations for each $i \in \mathcal{N}$:

$$\sum_{j\in\mathcal{N}} a_{ij}\hat{x}_j = \frac{\hat{x}_i}{\tau_1(1-\hat{x}_i-\hat{y}_i)}, \quad \sum_{j\in\mathcal{N}} b_{ij}\hat{y}_j = \frac{\hat{y}_i}{\tau_2(1-\hat{x}_i-\hat{y}_i)}. \tag{5}$$

Analyzing these equations by first trying to show the convexity of CE in the system parameters, as done in [14] for the single-virus SIS model, would be infeasible. This is because the second-order derivatives of the bi-SIS model quickly become intractable due to the highly coupled nature of the ODE system and its fixed point equations, as seen in (2) and (5) respectively. Instead, our approach is to first leverage the underlying monotonicity properties of the bi-SIS system. Apart from the bi-virus ODE system (2) being MDS [21], i.e., the trajectories of (2) preserving the ordering of the initial points, we show in the following lemma that the CE (which is the limiting state of the system) also exhibits strong monotonicity with respect to the effective infection rates τ_1 and τ_2.

Lemma 1. *Let* $(\hat{\mathbf{x}}, \hat{\mathbf{y}}) \gg (\mathbf{0}, \mathbf{0})$ *be a CE of the bi-SIS ODE* (2)*. For all* $i \in \mathcal{N}$*, entries* $\hat{x}_i$ *of* $\hat{\mathbf{x}}$ *increase in* τ_1 *(decrease in* τ_2*), while entries* $\hat{y}_i$ *of* $\hat{\mathbf{y}}$ *decrease in* τ_1 *(increase in* τ_2*). That is,*

$$\frac{\partial\hat{x}_i}{\partial\tau_1} > 0, \quad \frac{\partial\hat{y}_i}{\partial\tau_1} < 0, \quad \textit{and} \quad \frac{\partial\hat{x}_i}{\partial\tau_2} < 0, \quad \frac{\partial\hat{y}_i}{\partial\tau_2} > 0. \qquad \square$$

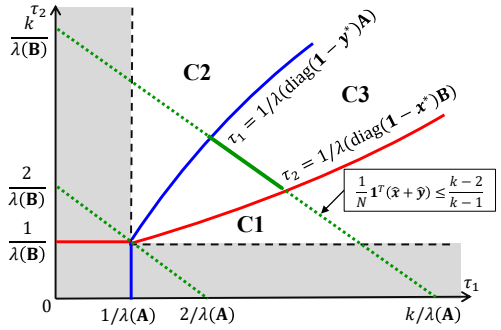

Fig. 1. The unshaded region is divided by blue curve and red curve (boundary conditions of τ_1, τ_2) into three parts, corresponding to (C1)-(C3) in Section II-B. The discussion on the equilibrium in the shaded region is deferred to our previous work [21]. Green solid-line is the set of system parameters (τ_1, τ_2) inside C3 such that they exhibit the same upper bound $(\mathbf{1}^T\hat{\mathbf{x}} + \mathbf{1}^T\hat{\mathbf{y}})/N \leq (k-2)/(k-1)$ for $k > 2$.

From Lemma 1, we can see that changes in $\hat{\mathbf{x}}$ and $\hat{\mathbf{y}}$, caused by perturbation to any of the system parameters, are always in the opposite direction. Moreover, changes in both $\hat{\mathbf{x}}_i$ and $\hat{\mathbf{y}}_i$ with respect to τ_1 and τ_2 are strict. This form of strong monotonicity helps us establish the following result, which better captures the coupled relationship of $\hat{\mathbf{x}}$ and $\hat{\mathbf{y}}$ with the system parameters in (5).

Theorem 1. *The term* $\hat{y}_i/(1-\hat{x}_i)$ *strictly decreases (increases) in* τ_1 *(*τ_2*),* $\forall i \in \mathcal{N}$*. Similarly, the term* $\hat{x}_i/(1-\hat{y}_i)$ *strictly increases (decreases) in* τ_1 *(*τ_2*),* $\forall i \in \mathcal{N}$*.* $\square$

Lemma 1 implies that $1/(1-\hat{x}_i)$ increases in τ_1 due to $\hat{x}_i$ increasing in τ_1, while $\hat{y}_i$ decreases in τ_1. However, their product $\hat{y}_i/(1-\hat{x}_i)$ may not possess any apparent monotonicity in τ_1, depending on the amount of increase and decrease observed by $\hat{x}_i$ and $\hat{y}_i$. Theorem 1 asserts that this term indeed decreases monotonically in τ_1, implying that the decrease in $1-\hat{x}_i$ is not large enough to offset that of $\hat{y}_i$ for all values of τ_1 in (C3). Thus, Theorem 1 is much sharper in capturing the coupled change in entries of $\hat{\mathbf{x}}$ and $\hat{\mathbf{y}}$ as the system parameters τ_1 and τ_2 are varied, and we are able to do this by combining Lemma 1 with careful analysis of the first order derivatives of the CE fixed point equations (5). We have the following corollary as a consequence of Theorem 1.

Corollary 1. *For each* $i \in \mathcal{N}$*, we have the inequalities*

$$\hat{x}_i < x^*_i(1-\hat{y}_i), \quad \hat{y}_i < y^*_i(1-\hat{x}_i). \qquad \square \tag{6}$$

To understand the implication of Corollary 1, we briefly consider the example of competing products (modelled as viruses). Where a new product (Product 1) enters a market, more often than not, there is another existing dominant product (Product 2) enjoying its own market share $\hat{\mathbf{y}} = \mathbf{y}^*$. Through mechanisms such as marketing techniques, the Product 1 increases its own influence τ_1, and eventually gains a foothold into the market $\hat{\mathbf{x}} \gg \mathbf{0}$. From Lemma 1, we can only guess that the market share $\hat{\mathbf{y}}$ would fall below its initial dominating value $\mathbf{y}^*$, but there is not much one can say in terms of quantifying the reduction in $\hat{\mathbf{y}}$.

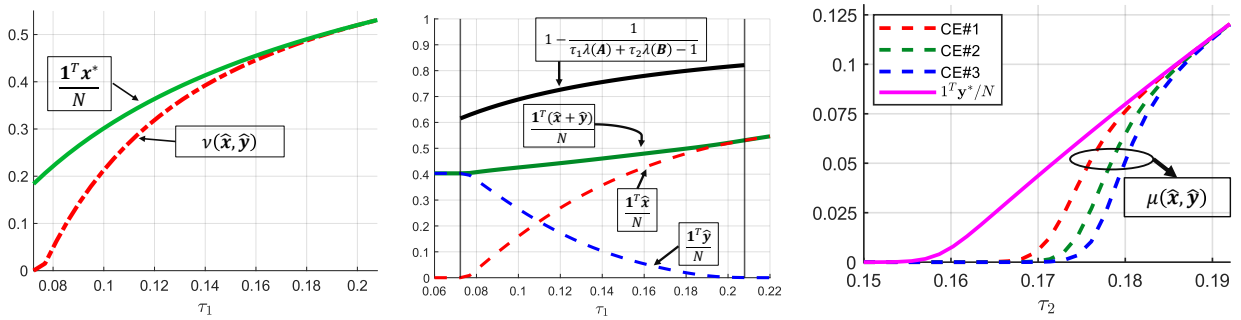

(a) Using AS-733-A and AS-733-B as overlaid graphs for Corollary 1.

(b) Using AS-733-A and AS-733-B as overlaid graphs for Proposition 2.

(c) Using AS-733-B and AS-733-C as overlaid graphs for Corollary 1 with three CE fixed points.

Fig. 2. Numerical results on the AS-733 graph.

From Corollary 1, we now know that at each node $i \in \mathcal{N}$, the influence of Product 1 $\hat{y}_i$ will fall by a factor of at least $(1-\hat{x}_i)$ compared to its original value of y_i^*. This is particularly useful when the competing viruses have access to the information about each others' local market share at each node. When this information is not available, we have the following proposition which decouples the complicated relationship between CE fixed points.

Proposition 2. *Let $(\hat{\mathbf{x}},\hat{\mathbf{y}})$ be a CE fixed point of the bi-SIS system* (2)*. Then, the average number of infected nodes in the network $(\mathbf{1}^T\hat{\mathbf{x}}+\mathbf{1}^T\hat{\mathbf{y}})/N$ is upper bounded as*

$$\frac{1}{N}(\mathbf{1}^T\hat{\mathbf{x}}+\mathbf{1}^T\hat{\mathbf{y}}) < 1-\frac{1}{\tau_1\lambda(\mathbf{A})+\tau_2\lambda(\mathbf{B})-1}. \qquad \square \ (7)$$

Suppose that $\tau_1\lambda(\mathbf{A})$ and $\tau_2\lambda(\mathbf{B})$ are only slightly larger than 1, implying (in light of condition (C3)) that quantities $\tau_1\lambda(\text{diag}(\mathbf{1}-\mathbf{y}^*)\mathbf{A})$ and $\tau_2\lambda(\text{diag}(\mathbf{1}-\mathbf{x}^*)\mathbf{B})$ are also only slightly larger than 1, and just barely satisfy the coexistence condition (C3) by a small margin. In this case, the average number of infected nodes $(\mathbf{1}^T\hat{\mathbf{x}}+\mathbf{1}^T\hat{\mathbf{y}})/N$ must also be small (albeit strictly positive), as would be expected. Note however that the upper bound in (7) holds for much larger values of τ_1,τ_2 as long as they satisfy the CE condition (C3). For instance in Figure 1, the green dash-line represents the set of all possible τ_1,τ_2 in the CE condition satisfying $\tau_1\lambda(\mathbf{A})+\tau_2\lambda(\mathbf{B})=k$ such that the upper bound remains the same for all the parameters in this (level) set. We also note that the upper bound in (7) holds for all possible (finitely many) CE fixed points. In addition, our bound on the CE decouples the cross-dependency of competing viruses on overlaid graphs, into *each* of single-SIS on its own graph (upper bound in (7) dependent only on the graphs, and not on $\mathbf{x}^*$ or $\mathbf{y}^*$). This will shed some light on how to fine-tune the system parameters τ_1,τ_2 or how tho modify the graph adjacency matrices $\mathbf{A},\mathbf{B}$ for some real-world applications, e.g, strategy design in the medical area in order to control the infection probability of either of two viruses with limited medical resources.

IV. Numerical Results

In this section, we present numerical results to assess the tightness of the upper bounds in Corollary 1 and Proposition 2. To this end, we consider an undirected, connected graph AS-733 from the SNAP repository [22] and generate three graphs with the same 103 nodes but with different edge sets, by modifying the edges of AS-733 while preserving the connectivity. The new graphs AS-733-A, AS-733-B and AS-733-C have 616, 267, and 297 edges, respectively. Table I summarizes the range of system parameters, chosen in a way to ensure that $\tau_1 > 1/\lambda(\mathbf{A})$ and $\tau_2 > 1/\lambda(\mathbf{B})$, i.e., the infection rates never lie in the gray region in Figure 1. We numerically solve the ODE system (2) for the chosen parameters until convergence is observed.

To capture how the upper bounds behave with change in system parameters, we fix τ_2 and vary τ_1 in Figure 2a, 2b. Denote by $\mu(\hat{\mathbf{x}},\hat{\mathbf{y}}) \triangleq (1/N)\sum_i \hat{y}_i/(1-\hat{x}_i)$, and $\nu(\hat{\mathbf{x}},\hat{\mathbf{y}}) \triangleq (1/N)\sum_i \hat{x}_i/(1-\hat{y}_i)$. In Figure 2a, the range of τ_1 and $\tau_2$values are under the CE condition. We can see that $\nu(\hat{\mathbf{x}},\hat{\mathbf{y}})$ is increasing in τ_1, as is expected from Theorem 1. In addition, $\nu(\hat{\mathbf{x}},\hat{\mathbf{y}})$ gets closer to the average infection probability of Virus 1 in the single-SIS case as τ_1 increases because Virus 1 becomes more dominant over Virus 2 and the bi-SIS ODE system (2) behaves similar to the single-virus system. For Figure 2b, as τ_1 increases over the range of values from the first row in Table I, the system parameters transit from regions (C1) to (C3) to (C2) of Figure 1; Virus 1 dies out for $\tau_1 \in [0.06, 0.072]$ while Virus 2 survives, both viruses survive for $\tau_1 \in (0.072, 0.208)$, and Virus 2 dies out while Virus 1 survives for $\tau_1 \in [0.208, 0.22]$. The upper bound (in black line) also captures the trend for the average probability of being infected by either virus and has good estimation as τ_1 increases.

Next, we fix τ_1 and vary τ_2, which is given in the second row in Table I, in order to see how τ_2, instead of τ_1, can affect $\mu(\hat{\mathbf{x}},\hat{\mathbf{y}})$ in Corollary 1. Unlike to Figure 2a and 2b that only contain single CE, we use AS-733-B and AS-733-C as overlaid graphs to show the existence of multiple CE fixed

τ_1 : 0.06 $\sim$ 0.22, τ_2 = 0.3173	$\lambda(\mathbf{A})$ = 22.13, $\lambda(\mathbf{B})$ = 6.3
τ_1 = 0.17, τ_2 : 0.15 $\sim$ 0.92	$\lambda(\mathbf{C})$ = 6.59, $\lambda(\mathbf{B})$ = 6.3

TABLE I
System Parameters

points in Figure 2c, which all satisfy (6) in Corollary 1. The curves in Figure 2c also share the similar trend in Figure 2a that the upper bound becomes tight for large τ_2.

V. Conclusion

In this paper we have provided, for the first time, quantitative results on the coexistence equilibria of bi-SIS epidemic models for general graphs. A future direction can include similar analysis for graphs with special topologies such as star, and line graphs, as well as cases such as ER random graphs, for which one could potentially obtain tighter results than those in Section III which were presented for general graphs.

References

[1] F. Darabi Sahneh, C. Scoglio, and P. Van Mieghem, "Generalized epidemic mean-field model for spreading processes over multilayer complex networks," *IEEE/ACM Transactions on Networking*, vol. 21, no. 5, pp. 1609–1620, 2013.

[2] A. Janson, S. Gracy, P. E. Paré, H. Sandberg, and K. H. Johansson, "Networked Multi-Virus Spread with a Shared Resource: Analysis and Mitigation Strategies," *ArXiv*, vol. abs/2011.07569, 2020.

[3] P. E. Paré, J. Liu, C. L. Beck, A. Nedić, and T. Başar, "Multi-competitive viruses over time-varying networks with mutations and human awareness," *Autom.*, vol. 123, p. 109330, 2021.

[4] S. F. Ruf, K. Paarporn, P. E. Pare, and M. Egerstedt, "Dynamics of opinion-dependent product spread," in *IEEE Conference on Decision and Control*, Melbourne, Australia, 2017.

[5] K. R. Apt and E. Markakis, "Diffusion in social networks with competing products," in *International Symposium on Algorithmic Game Theory*, 2011.

[6] B. A. Prakash, A. Beutel, R. Rosenfeld, and C. Faloutsos, "Winner takes all: competing viruses or ideas on fair-play networks," in *ACM World Wide Web*, 2012.

[7] J. Liu, P. E. Paré, A. Nedić, C. Y. Tang, C. L. Beck, and T. Başar, "On the analysis of a continuous-time bi-virus model," in *IEEE Conference on Decision and Control*, Las Vegas, NV, 2016.

[8] M. Ye, B. Anderson, and J. Liu, "Convergence and equilibria analysis of a networked bivirus epidemic model," *arXiv:2111.07507*, 2021.

[9] F. D. Sahneh and C. Scoglio, "Competitive epidemic spreading over arbitrary multilayer networks," *Physical Review E*, vol. 89, no. 6, p. 062817, 2014.

[10] L.-X. Yang, X. Yang, and Y. Y. Tang, "A bi-virus competing spreading model with generic infection rates," *IEEE Transactions on Network Science and Engineering*, vol. 5, no. 1, pp. 2–13, 2017.

[11] A. Santos, J. M. F. Moura, and J. M. F. Xavier, "Bi-virus SIS epidemics over networks: Qualitative analysis," *IEEE Transactions on Network Science and Engineering*, vol. 2, no. 1, pp. 17–29, 2015.

[12] A. Lajmanovich and J. A. Yorke, "A deterministic model for gonorrhea in a nonhomogeneous population," *Mathematical Biosciences*, vol. 28, no. 3, pp. 221 – 236, 1976.

[13] C. Castellano and R. Pastor-Satorras, "Thresholds for Epidemic Spreading in Networks," *Phys. Rev. Lett.*, vol. 105, p. 218701, Nov 2010.

[14] P. Mieghem and J. Omic, "In-homogeneous Virus Spread in Networks," *arXiv:1306.2588*, 06 2013.

[15] P. Van Mieghem, J. Omic, and R. Kooij, "Virus spread in networks," *IEEE/ACM Transactions on Networking*, vol. 17, no. 1, pp. 1–14, 2009.

[16] P. Van Mieghem, "The Viral Conductance of a Network," *Comput. Commun.*, vol. 35, no. 12, p. 1494–1506, Jul 2012.

[17] ——, "The n-intertwined sis epidemic network model," *Computing*, vol. 93, no. 2, pp. 147–169, 2011.

[18] A. Gray, D. Greenhalgh, L. Hu, X. Mao, and J. Pan, "A stochastic differential equation SIS epidemic model," *SIAM Journal on Applied Mathematics*, vol. 71, no. 3, pp. 876–902, 2011.

[19] C. Li, R. van de Bovenkamp, and P. Van Mieghem, "Susceptible-infected-susceptible model: A comparison of n-intertwined and heterogeneous mean-field approximations," *Physical Review E*, vol. 86, no. 2, p. 026116, 2012.

[20] U. Krause and P. Ranft, "A limit set trichotomy for monotone nonlinear dynamical systems," *Nonlinear Analysis: Theory, Methods & Applications*, vol. 19, no. 4, pp. 375 – 392, 1992.

[21] V. Doshi, S. Mallick, and D. Y. Eun, "Competing Epidemics on Graphs - Global Convergence and Coexistence," in *IEEE INFOCOM*, 2021.

[22] J. Leskovec and A. Krevl, "Snap datasets: Stanford large network dataset collection," 2014.

[23] C. M. Fortuin and J. Ginibre and P. W. Kasteleyn, "Correlation inequalities on some partially ordered sets," *Communications in Mathematical Physics*, vol. 22, no. 2, pp. 89 – 103, 1971.

[24] C. D. Meyer, *Matrix analysis and applied linear algebra*. Siam, 2000.

Appendix I
Proofs of results

Proof: [Proof of Proposition 1] By considering the i-th entry in (3) and setting $dx_i/dt = 0$, we obtain the fixed point equation

$$\sum_{j\in\mathcal{N}} a_{ij}x_j^* = \frac{1}{\tau}\frac{x_i^*}{1-x_i^*}. \tag{8}$$

From the min-max theorem, we write $\lambda(\mathbf{A})$ in the Rayleigh quotient form such that

$$\lambda(\mathbf{A}) = \max_{\mathbf{y}\neq\mathbf{0}} \frac{\mathbf{y}^T\mathbf{A}\mathbf{y}}{\mathbf{y}^T\mathbf{y}} \geq \frac{(\mathbf{x}^*)^T\mathbf{A}\mathbf{x}^*}{(\mathbf{x}^*)^T\mathbf{x}^*} = \frac{\sum\limits_{i\in\mathcal{N}} x_i^* \sum\limits_{j\in\mathcal{N}} a_{ij}x_j^*}{\sum\limits_{i\in\mathcal{N}}(x_i^*)^2}. \tag{9}$$

where the inequality comes from picking $\mathbf{y} = \mathbf{x}^*$ and the second equality is by rewriting the matrix multiplication in the summation notation. Define a random variable Y which takes values x_i^* with probability $1/N$ for all $i \in \mathcal{N}$, and $\mathbb{E}[Y] = \mathbf{1}^T\mathbf{x}^*/N$. Then, replacing $\sum_{j\in\mathcal{N}} a_{ij}x_j^*$ in (9) with (8) gives

$$\lambda(\mathbf{A}) \geq \frac{\frac{1}{N}\sum_{i\in\mathcal{N}}(x_i^*)^2/(1-x_i^*)}{\tau\frac{1}{N}\sum_{i\in\mathcal{N}}(x_i^*)^2} = \frac{\mathbb{E}[Y^2/(1-Y)]}{\tau\mathbb{E}[Y^2]}. \tag{10}$$

Since Y^2 and $1/(1-Y)$ are both increasing functions in $Y \in (0,1)$, FKG inequality [23] gives $\mathbb{E}[Y^2/(1-Y)] \geq \mathbb{E}[Y^2]\mathbb{E}[1/(1-Y)]$. Then, from (10) we have

$$\tau\lambda(\mathbf{A}) \geq \frac{\mathbb{E}[Y^2]\mathbb{E}[1/(1-Y)]}{\mathbb{E}[Y^2]} = \mathbb{E}\left[\frac{1}{1-Y}\right] \geq \frac{1}{1-\mathbb{E}[Y]}, \tag{11}$$

where the second inequality comes from Jensen's inequality. Rearranging (11) gives (4).

We denote $\mathbb{R}_+$ the set of all positive real numbers. Then, with the Collatz-Wielandt formula [24], we rewrite $\lambda(\mathbf{A})$ as

$$\lambda(\mathbf{A}) = \min_{\mathbf{y}\in\mathbb{R}_+^N} \max_{i\in\mathcal{N}} \frac{[\mathbf{A}\mathbf{y}]_i}{y_i} \leq \max_{i\in\mathcal{N}} \frac{[\mathbf{A}\mathbf{x}^*]_i}{x_i^*} = \frac{1}{\tau(1-x_{\max})}, \tag{12}$$

where the inequality is from choosing $\mathbf{y} = \mathbf{x}^*$. The second equality in (12) comes from (8). Then, rearranging (12) gives $x_{\max} \geq 1 - 1/\tau\lambda(\mathbf{A})$. □

Proof: [Proof of Lemma 1] We only present the proof for the behaviour of $\hat{\mathbf{x}}$ and $\hat{\mathbf{y}}$ in τ_1, since the case involving τ_2 follows by symmetry. Consider the bi-SIS model

$$\begin{aligned} \dot{\mathbf{x}} &= (\beta_1+\epsilon)\text{diag}\,(\mathbf{1}-\mathbf{x}-\mathbf{y})\,\mathbf{A}\mathbf{x} - \delta_1\mathbf{x} \\ \dot{\mathbf{y}} &= \beta_2\text{diag}\,(\mathbf{1}-\mathbf{x}-\mathbf{y})\,\mathbf{B}\mathbf{y} - \delta_2\mathbf{y}, \end{aligned} \tag{13}$$

where we use ϵ as the parameter to vary τ_1. It is enough to show that entries $\hat{x}_i$ of $\hat{\mathbf{x}}$ ($\hat{y}_i$ of $\hat{\mathbf{y}}$) increase (decrease) in ϵ.[4].

We now consider trajectories of system (13) starting from $(\hat{\mathbf{x}}, \hat{\mathbf{y}})$. Note that by definition $(\hat{\mathbf{x}}, \hat{\mathbf{y}}) \gg (\mathbf{0}, \mathbf{0})$ is a fixed point of the system when $\epsilon = 0$, and in this case we have $\dot{\mathbf{x}} =$

[4]Instead of $\beta_1+\epsilon$, we could also vary τ_1 by replacing δ_1 with $\delta-\epsilon$. The steps remain similar, with both methods leading to the same conclusion.

0 and $\dot{\mathbf{y}} = 0$. However for any $\epsilon > 0$, we have $\dot{\mathbf{x}} \gg \mathbf{0}$ and $\dot{\mathbf{y}} = \mathbf{0}$. Let $\phi_t(\mathbf{x}, \mathbf{y}) \in [0,1]^2 N$ denote the flow of the system at time $t > 0$, with initial point $(\mathbf{x}, \mathbf{y}) \in D$, with $\phi_t^x(\mathbf{x}, \mathbf{y}) \in [0,1]^N$ corresponding to the the infection probabilities for Virus 1, and $\phi_t^y(\mathbf{x}, \mathbf{y}) \in [0,1]^N$ corresponding to those of Virus 2. Then for any $\epsilon > 0$ sufficiently small $s > 0$ we have $\phi_s^x(\hat{\mathbf{x}}, \hat{\mathbf{y}}) > \phi_0^x(\hat{\mathbf{x}}, \hat{\mathbf{y}}) = \hat{\mathbf{x}}$, and $\phi_s^y(\hat{\mathbf{x}}, \hat{\mathbf{y}}) = \phi_0^y(\hat{\mathbf{x}}, \hat{\mathbf{y}}) = \hat{\mathbf{y}}$.

As a consequence of Proposition 3.1 in [21], the bi-SIS system is considered to be *strongly monotone* in $\text{Int}(D)$.[5] The result is that $\phi_{t+s}^x(\hat{\mathbf{x}}, \hat{\mathbf{y}}) \gg \mathbf{x}$, and $\phi_{t+s}^y(\hat{\mathbf{x}}, \hat{\mathbf{y}}) \ll \mathbf{y}$ for all $t > 0$. For any $\epsilon > 0$, let $(\hat{\mathbf{x}}_\epsilon, \hat{\mathbf{y}}_\epsilon) \triangleq \lim_{t\to\infty} \phi_t(\hat{\mathbf{x}}, \hat{\mathbf{y}})$ denote the convergent point of trajectory starting from $(\hat{\mathbf{x}}, \hat{\mathbf{y}})$. Since we consider only small enough $\epsilon > 0$ that still satisfying the coexistence conditions (C3), the point $(\hat{\mathbf{x}}_\epsilon, \hat{\mathbf{y}}_\epsilon) \gg (\mathbf{0}, \mathbf{0})$ is now the CE fixed point corresponding to the choice of $\epsilon > 0$, and satisfies $\hat{\mathbf{x}}_\epsilon \gg \hat{\mathbf{x}}$ and $\hat{\mathbf{y}}_\epsilon \ll \hat{\mathbf{y}}$. By similar arguments, the reverse holds true when $\epsilon < 0$, while still satisfying conditions (C3), that is the trajectories starting from $(\hat{\mathbf{x}}, \hat{\mathbf{y}})$ converge to another CE fixed point such that $\hat{\mathbf{x}}_\epsilon \ll \hat{\mathbf{x}}$ and $\hat{\mathbf{y}}_\epsilon \gg \hat{\mathbf{y}}$.

Therefore, for all system parameters τ_1, τ_2 satisfying coexistence conditions (C3), and lying within the corresponding region in Figure 1, the entries of $\hat{\mathbf{x}}$ increase (entries of $\hat{\mathbf{y}}$ decrease) in τ_1 for any CE. This completes the proof. □

Proof: [Proof of Theorem 1] Let $f_i \triangleq \hat{y}_i/(1-\hat{x}_i)$ and $g_i \triangleq \hat{x}_i/(1-\hat{y}_i)$ for notation simplicity. We only prove that f_i is decreasing (increasing) in τ_1 (τ_2), since the similar result for g_i follows by a symmetric argument.

We use the notation by $[\partial\hat{y}_i/\partial\hat{x}_j]_{\tau_1} \triangleq \frac{\partial\hat{y}_i/\partial\tau_1}{\partial\hat{x}_j/\partial\tau_1}$ to denote the change in $\hat{y}_i$ with respect to change $\hat{x}_i$ due to increase or decrease in τ_1. Similarly, we use the notation $[\partial\hat{x}_i/\partial\hat{y}_j]_{\tau_2}$ to denote the change in $\hat{x}_i$ with respect to change in $\hat{y}_i$ due increase or decrease in τ_2. We first prove the following:

$$\left[\frac{\partial\hat{y}_i}{\partial\hat{x}_i}\right]_{\tau_1} < -\frac{\hat{y}_i}{1-\hat{x}_i}, \quad \left[\frac{\partial\hat{y}_i}{\partial\hat{x}_i}\right]_{\tau_2} < -\frac{\hat{y}_i}{1-\hat{x}_i} \tag{14}$$

Taking partial derivative of the logarithm of $\sum_j b_{ij}\hat{y}_j$ in the fixed point equation (5) with respect to τ_2, we obtain

$$\frac{1}{\sum_{j\in\mathcal{N}} b_{ij}\hat{y}_j}\sum_{j\in\mathcal{N}} b_{ij}\frac{\partial\hat{y}_j}{\partial\tau_2} = \frac{\partial\hat{y}_i}{\partial\tau_2}\left(\frac{1}{\hat{y}_i} + \frac{1+\left[\frac{\partial\hat{x}_i}{\partial\hat{y}_i}\right]_{\tau_2}}{1-\hat{x}_i-\hat{y}_i} - \frac{\partial\tau_2}{\tau_2\partial\hat{y}_i}\right). \tag{15}$$

The left-hand side of (15) is positive since $b_{ij} \geq 0$, $\hat{x}_j \in (0,1)$, and $\partial\hat{y}_j/\partial\tau_2 > 0$ in Lemma 1 for all $i, j \in \mathcal{N}$. Then, we have

$$0 < \frac{1}{\hat{y}_i} + \frac{1+\left[\frac{\partial\hat{x}_i}{\partial\hat{y}_i}\right]_{\tau_2}}{1-\hat{y}_i-\hat{x}_i} - \frac{1}{\tau_2\partial\hat{y}_i/\partial\tau_2} < \frac{1}{\hat{y}_i} + \frac{1+\left[\frac{\partial\hat{x}_i}{\partial\hat{y}_i}\right]_{\tau_2}}{1-\hat{x}_i-\hat{y}_i}, \tag{16}$$

where the first inequality is from the positivity of the terms in (15), and the second equality comes be removing the third summand, which we can do since $\partial\hat{y}_i/\partial\tau_2 > 0$ from Lemma 1. Then, rearranging (16) with respect to $[\partial\hat{y}_i/\partial\hat{x}_i]_{\tau_2}$ gives us $[\partial\hat{y}_i/\partial\hat{x}_i]_{\tau_2} < -\hat{y}_i/(1-\hat{x}_i)$. Performing the same steps by differentiating by the logarithm of the fixed point equation by τ_1 instead of τ_2 gives us $[\partial\hat{y}_i/\partial\hat{x}_i]_{\tau_1} < -\hat{y}_i/(1-\hat{x}_i)$, proving (14). Now, in order to show f_i is strictly decreasing in $\tau_1 > \tau_1^*$, it is enough to show $\partial f_i/\partial\tau_1 < 0$. Taking partial derivative of f_i with respect to τ_1 gives

$$\frac{\partial f_i}{\partial\tau_1} = \frac{(1-\hat{x}_i)\frac{\partial\hat{y}_i}{\partial\tau_1} + \hat{y}_i\frac{\partial\hat{x}_i}{\partial\tau_1}}{(1-\hat{x}_i)^2} = \frac{\partial\hat{x}_i}{\partial\tau_1}\cdot\frac{(1-\hat{x}_i)\left[\frac{\partial\hat{y}_i}{\partial\hat{x}_i}\right]_{\tau_1} + \hat{y}_i}{(1-\hat{x}_i)^2}. \tag{17}$$

The first inequality of (14) gives $(1-\hat{x}_i)\left[\partial\hat{y}_i/\partial\hat{x}_i\right]_{\tau_1} + \hat{y}_i < 0$. Together with $\partial\hat{x}_i/\partial\tau_1 > 0$ from Lemma 1, we can see from (17) that $\partial f_i/\partial\tau_1 < 0$ for all $i \in \mathcal{N}$. Similarly, we have

$$\frac{\partial f_i}{\partial\tau_2} = \frac{\partial\hat{x}_i}{\partial\tau_2}\cdot\frac{(1-\hat{x}_i)\left[\frac{\partial\hat{y}_i}{\partial\hat{x}_i}\right]_{\tau_2} + \hat{y}_i}{(1-\hat{x}_i)^2} > 0 \tag{18}$$

because $\partial\hat{x}_i/\partial\tau_2 < 0$ from Lemma 1, showing that f_i is strictly increasing in τ_2 for all $i \in \mathcal{N}$. □

Proof: [Proof of Corollary 1] We follow the notations $f_i \triangleq \hat{y}_i/(1-\hat{x}_i)$ and $g_i \triangleq \hat{x}_i/(1-\hat{y}_i)$ and assume the coexistence condition $\tau_1 > 1/\lambda(\text{diag}(\mathbf{1}-\mathbf{y}^*)\mathbf{A})$ and $\tau_2 > 1/\lambda(\text{diag}(\mathbf{1}-\mathbf{x}^*)\mathbf{B})$.

If $\tau_1 \leq 1/\lambda(\text{diag}(\mathbf{1}-\mathbf{y}^*)\mathbf{A})$, then virus 1 will die out, i.e., $\hat{x}_i = 0, \hat{y}_i = y_i^*$ and $f_i = y_i^*$ for all $i \in \mathcal{N}$. Since f_i is decreasing in $\tau_1 > 1/\lambda(\text{diag}(\mathbf{1}-\mathbf{y}^*)\mathbf{A})$, we have $f_i < y_i^*$.

Similarly, if $\tau_2 \leq 1/\lambda(\text{diag}(\mathbf{1}-\mathbf{x}^*)\mathbf{B})$, Virus 2 will die out, i.e., $\hat{y}_i = 0, \hat{x}_i = x_i^*$ and $g_i = x_i^*$ for all $i \in \mathcal{N}$. Since g_i is decreasing in $\tau_2 > 1/\lambda(\text{diag}(\mathbf{1}-\mathbf{x}^*)\mathbf{B})$, we have $g_i < x_i^*$. □

Proof: [Proof of Proposition 2] We first quantify the upper bound of $\hat{y}_i + \hat{x}_i$, $\forall i \in \mathcal{N}$. Rearranging (6) gives

$$\hat{y}_i < \min\left\{y_i^*(1-\hat{x}_i), 1-\hat{x}_i/x_i^*\right\}. \tag{19}$$

Then, adding $\hat{x}_i$ on both sides in (19) gives

$$\hat{y}_i + \hat{x}_i < \min\left\{y_i^*(1-\hat{x}_i) + \hat{x}_i, 1-\hat{x}_i/x_i^* + \hat{x}_i\right\}. \tag{20}$$

Note that $\hat{y}_i \in [0, y_i^*], \hat{x}_i \in [0, x_i^*]$ and $y_i^*, x_i^* \leq 1$, ensuring that the right-hand side term in (20) is concave in $\hat{x}_i \in [0, x_i^*]$. Then, the maximum of the upper bound in (20) is obtained by solving $y_i^*(1-\hat{x}_i) + \hat{x}_i = 1-\hat{x}_i/x_i^* + \hat{x}_i$ in terms of $\hat{x}_i$, which gives us $\hat{x}_i = (x_i^* - y_i^* x_i^*)/(1-y_i^* x_i^*)$. Putting this expression back to (20) leads to $\hat{y}_i + \hat{x}_i < (x_i^* + y_i^* - 2x_i^* y_i^*)/(1-x_i^* y_i^*)$, or equivalently,

$$1-\hat{y}_i-\hat{x}_i > \frac{(1-x_i^*)(1-y_i^*)}{1-x_i^* y_i^*} = \frac{1}{\frac{1}{1-x_i^*} + \frac{1}{1-y_i^*} - 1}. \tag{21}$$

Note that $\mathbf{x}^*, \mathbf{y}^*$ are unrelated to each other because they are the fixed points in the single-virus SIS case where the other virus dies out. We define two independent random variables X, Y that take values x_i^*, y_i^* with probability $1/N$ for all $i \in \mathcal{N}$. From (11), we have

$$\tau_1\lambda(\mathbf{A}) \geq \mathbb{E}[1/(1-X)], \quad \tau_2\lambda(\mathbf{B}) \geq \mathbb{E}[1/(1-Y)]. \tag{22}$$

We also define a random variable Z that takes values $1/(1-x_i^*) + 1/(1-y_i^*)$ with probability $1/N$ for all $i \in \mathcal{N}$, and $\mathbb{E}[Z] = \mathbb{E}[1/(1-X)] + \mathbb{E}[1/(1-Y)]$. From (22), we have

$$\mathbb{E}[Z] \geq \tau_1\lambda(\mathbf{A}) + \tau_2\lambda(\mathbf{B}). \tag{23}$$

Then, summing (21) over all $i \in \mathcal{N}$ and dividing by N gives

$$\frac{1}{N}\sum_{i\in\mathcal{N}}(1-\hat{y}_i-\hat{x}_i) > \frac{1}{N}\sum_{i\in\mathcal{N}}\frac{1}{\frac{1}{1-x_i^*} + \frac{1}{1-y_i^*} - 1} = \mathbb{E}\left[\frac{1}{Z-1}\right].$$

Using Jensen's inequality in the above leads to

$$\frac{1}{N}\sum_{i\in\mathcal{N}}(1-\hat{y}_i-\hat{x}_i) > \frac{1}{\mathbb{E}[Z]-1} \geq \frac{1}{\tau_1\lambda(\mathbf{A}) + \tau_2\lambda(\mathbf{B}) - 1}, \tag{24}$$

where the last inequality comes from (23). Rearranging (24) completes the proof. □

[5] A short educational primer on MDS is included in [21].